International Journal of Recent Technology and Engineering (IJRTE)
ISSN: 2277-3878 (Online), 4 Issue-6, January 2016

Low Velocity Impact Damage Analysis in Plain Weave Woven GFRP Laminates Through Optical and SEM Microscopy

M. A. Kounain, Z. Khan, F. Al-Sulaiman, N. Merah

Abstract: ***In the present study, instrumented drop weight impact tests at different impact energies were performed to investigate the modes and mechanisms of the low velocity impact damage in plain weave woven glass fiber reinforced plastic (GFRP) composite laminates. 8-ply, 16-ply, 24-ply and 32-ply laminates having identical 0^o layup were examined via optical and scanning electron microscopy after free falling weight single bounce impacts. It was found that under low velocity impact the failure was initiated by matrix cracking at the interstitial region of 0° GFRP composite laminates. These matrix cracks were much extensive in 8-ply laminates as compared to laminates with larger number of plies. These matrix cracks propagate to cause fiber fracture and fiber matrix debonding and extend across the thickness of the laminate to introduce delamination. The eventual failure thus occurs through the combination of matrix cracking, fiber fracture, fiber matrix debonding and delamination.***

Keywords: Low Velocity Impact, GFRP Laminates, Damage Characterization, Optical and SEM Microscopy

I. INTRODUCTION

Characterization of impact damage in glass fiber reinforced plastic composites has been the subject of considerable concern for a number of years. Several important issues regarding the impact damage evaluation, post damage effects, and damage modeling has been addressed in recent past. However, until now low velocity impact damage characterization and its effect on residual mechanical properties has not been considered fully. Engineers, designers, and manufacturers are still lacking availability of useful and reliable engineering data on damage tolerance, damage mechanics, damage mechanisms, and damage modeling in GFRP subjected to low velocity impact. Low velocity impact normally involves deformation of the entire structure during the contact duration of the impactor, and this situation is considered quasi-static with no consideration of the stress waves that propagate between the impactor and the boundary of the impacted component.

Revised Manuscript Received on 30 January 2016.
***** Correspondence Author
M. A. Kounain*, Technology Transfer, Innovation and Entrepreneurship Office, King Fahd University of Petroleum and Minerals, Dhahran, Saudi Arabia.
Z. Khan, Professor, Mechanical Engineering Department, King Fahd University of Petroleum and Minerals, Dhahran, Saudi Arabia.
Faleh Al-Sulaiman, CEO, National Company of Mechanical Systems, Riyadh, Saudi Arabia.
N. Merah, Professor, Mechanical Engineering Department, King Fahd University of Petroleum and Minerals, Dhahran, Saudi Arabia.

The effect of low-velocity impact damage on the FRP composites laminates and pipes has been studied by a number of researchers over the past several years [1-5]. Metallographic examination of the cross sections of the impact tested E-glass fabrics, non-crimp fabric, woven fabric reveal that fiber breakage had occurred prior to the major damage. When the impact energy increased over the threshold energy of the major damage, matrix cracking, delamination, and fiber breakage were observed at the back surface, below a nearly undamaged zone, which were attributed to the bending stresses [6]. The authors concluded that the first drop in the load-time plot corresponds to the matrix cracking. Composite plates fabricated and subjected to low-velocity impact revealed that the delamination area was proportional to the lamina thickness and the difference of fiber angle between adjacent laminae. It was found that through-the-thickness stitching could reduce the delamination area in a composite plate subjected to low-velocity impact as high as 40% [7]. Another investigation [8] examined low-velocity impact damage in cross-ply E-glass/epoxy laminated composite plates with a vertical drop-weight testing machine at two different tup weights of 1.35 kg and 2.6 kg. It was shown that the damage initiation occurs by matrix cracking. These cracks then generate delamination immediately along the top or bottom interface of the cracked layer. Morais et al. [9] explored the variation of the resistance to low energy repeated impacts of glass, carbon, and aramid fabrics-reinforced composites as a function of the laminate thickness. It was found that the front face shows dome fracture, resulting from the localized matrix crushing and fiber shearing under the indentator. At the rear face, the damage shows a characteristic pattern of cracks in the fiber direction of the fabrics. The authors concluded that the main damage occurs through fiber deformation and rupture. Dear and Brown [10] investigated the impact behavior of two grades of Sheet molding compound (SMC) and one grade of glass mat thermoplastic (GMT). The authors reported that the onset of through-thickness damage could occur before there was a visual evidence of surface damage at the point of contact between the striker and the specimen. A linear relationship has been observed between impact energy absorbed and peak load. The results showed that the composite with higher glass fiber weight fraction absorbs most impact energy. The materials exhibited the same propensity to have well-hidden through-thickness impact damage before damage to the front and rear faces was visible. Chang and Choi [11] investigated impact failure in a carbon fiber reinforced epoxy under low velocity impact loading and showed that matrix cracking can trigger delamination at neighboring ply interfaces in composite laminates.

Zhou [12] conducted low velocity impact tests on a glass fiber reinforced composite using a blunt indentor. He showed that delamination, fiber fracture and fiber shear out are the predominant mechanisms for absorbing kinetic energy and determining the load-bearing capability of the laminate. The main aim of the reported work is to present and discuss the damage developed during the low-velocity impact in plain weave woven glass fiber/epoxy matrix laminates through optical and Scanning Electron Microscopy analyses. The modes and mechanisms of impact damage have been identified. The effect of number of laminate plies (or laminate thickness) on the impact damage modes and mechanism has been explained.

II. MATERIAL AND METHODS

II-1 Specimen Fabrication

8-ply, 16-ply, 24-ply and 32-ply laminates, all having an identical 0^o orientation, were fabricated using a hand layup and vacuum bagging process. Glass fiber glue was used as resin which accounted to 150% of fiber weight. Polyester stitch yarns were used in the weft direction to hold the glass fibers. The volume fraction of glass fibers in the prepreg fabrics was approximately 65%. Table 1 shows the thickness and density of the investigated laminates.

Table 1 Material configuration of Woven Composite laminates

Specimen	Average Thickness (cm)	Density (g/cm^3)
0^0 8 Ply	0.097	1.34
0^0 16 Ply	0.2045	1.22
0^0 24 Ply	0.271	1.25
0^0 32 Ply	0.3845	1.15

II-2 Impact Testing

All impact tests were performed using an instrumented drop weight testing machine (Dynatup 9250G, Instron Corp., USA) at impact energies of 5, 7.5 and 10J. Impact energy was varied by the adjusting the height and mass of the falling hemispherical (10 mm dia.) steel tup impactor. The impact tests were performed on 150 mm x 150 mm specimens which were mounted on a steel fixture to receive single bounce impacts from the free falling impactor.

II-3 Impact Damage Analysis

Local observations of front (impacted) and opposite (rear) surfaces of impact damaged GFRP laminates were made using a low magnification metallographic microscope. These observations permitted macroscopic examination of the shape and extent of the impact damage including delamination and fiber fracture. In addition to the above observations, polished cross-sections of impact damage specimens are observed under microscope. For this, specimens were sectioned perpendicularly through the center of the impact damage zone and polishing the cross section down to 0.3 µm aluminum oxide surface finish. The cross sections were then observed under a low magnification metallographic microscope to examine the nature of through thickness impact damage. The surface morphology of impact damaged GFRP laminates was studied using Scanning Electron Microscope (SEM). 38 mm x 38 mm samples were cut from the impacted zones for SEM examination. To suppress charging and to increase electron emission, gold coating under vacuum was applied to the sample surface using ion sputter coating apparatus.

III. RESULTS AND DISCUSSION

8-Ply Laminates: Images of impact damage areas developed at different impact energies on the front (impacted) and the back (rear) side of [0o]8 laminates are shown in Figure . It is observed that the damage area increases with the increase in the impact energy. Unlike non-woven composite where the impact damage assumes a peanut shape, an X-shaped damage developed in the woven GFRP laminates as observed in Figure 2. The end points of the X-shaped damage seem to lie in the warp and weft strand directions. The region near the impact point on the composite exhibits fiber crushing (see Figure 2). This localized deformation is due to the high compressive stress generated close to the point of impact. At higher impact energy the [0o]8 laminates exhibit uniform deformation by the formation of dome shape as shown in Figure (c). Micrographs of impact damage at various magnifications taken using SEM are shown in Figure and Figure 4.

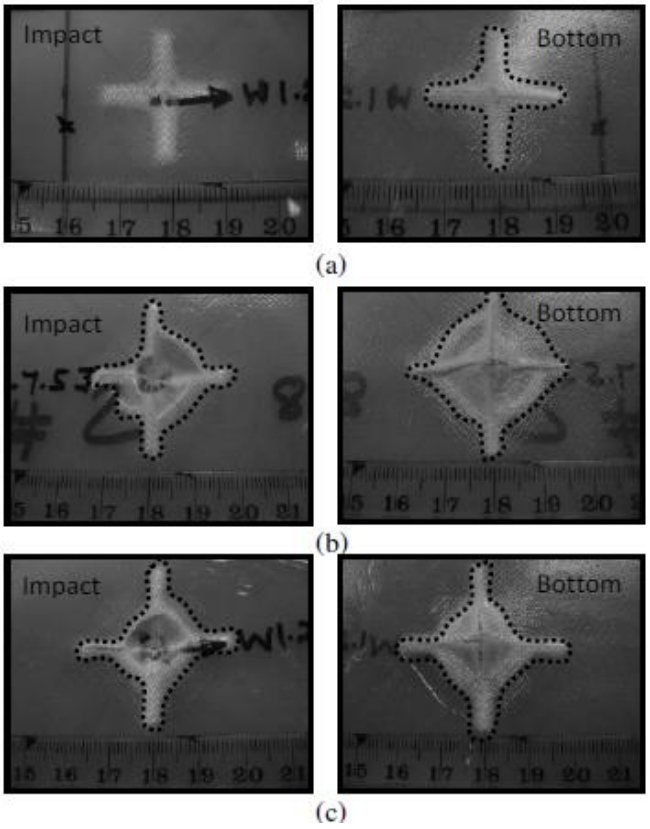

Figure 1. Impact and bottom side of the damage surface of $[0°]_8$ Specimen impacted at (a) 5J (b) 7.5J (c) 10J

These SEM micrographs show that the major failure in the laminate occurs through mode II delamination i.e. in a non-penetrating impact load are fiber/matrix interface debonding and matrix cracks (fracture of matrix) as observed in Figure2 (b), (c) and **Figure** (a). Shear stress developed due to impact load drives debonding and the delamination initiates from micro-cracks originating from the regions of fiber debonding.

Published By:
Blue Eyes Intelligence Engineering
and Sciences Publication (BEIESP)

Another impact damage mechanism the *fiber fracture* is observed in **Figure** and Figure . Fiber fracture/breakage when the material is impacted with a higher impact energy/load, higher stresses are developed in the material occurs when the impact load is sufficient to create stresses exceeding the fiber flexural strength. So which implies higher damage i.e. the amount of fiber fracture increases with the increase in impact energy.

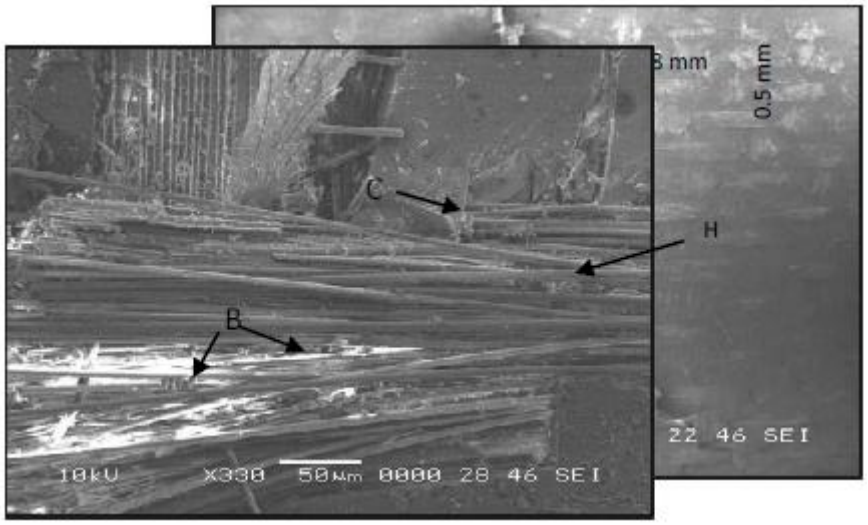

(b)

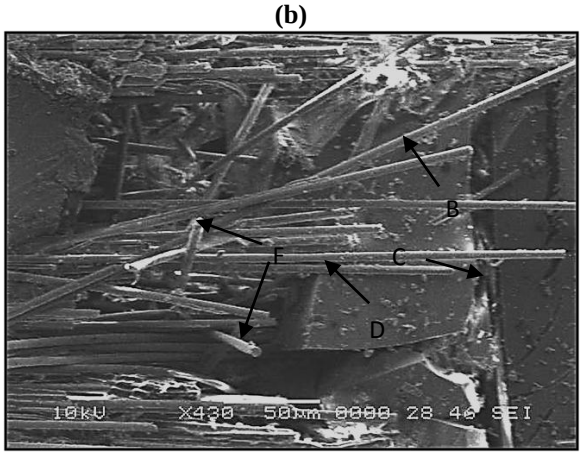

(c)

Figure 2. SEM micrographs of $[0°]_8$ specimen impacted at 5J showing Hackles (H), Matrix Cracking (C), Debonding (B), Fiber Fracture (E) and Delamination (D)

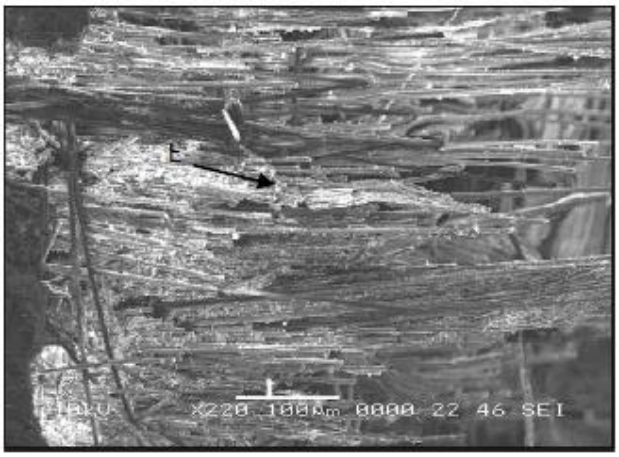

(a)

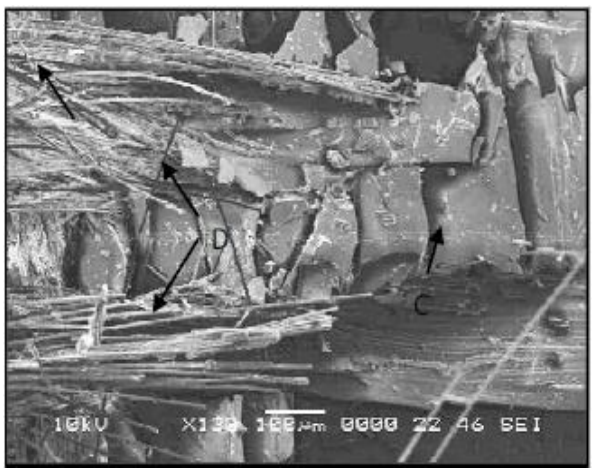

(b)

Figure 3. SEM micrographs of $[0°]_8$ specimen impacted at 7.5J showing Fiber Fracture (E), Delamination (D), Matrix Cracking (c)

It is known from previous research [**Error! Reference source not found.**13] that there are two distinct crack paths in a woven composite. The crack from weft to warp yarn can propagate through the matrix region (path A) and the fiber/matrix interface (path B) as show in Figure .

Published By:
Blue Eyes Intelligence Engineering and Sciences Publication (BEIESP)

Fracture surface of warp yarn region of woven glass fabric composite can be observed in Figure . It is known that when the crack propagates through path A, matrix material shows hackle pattern whereas in path B it is difficult to find the pattern. In this study no hackle patterns were identified in the above micrographs which mean that the crack had propagated through path B i.e. when the crack reaches warp yarn it goes over the yarn with the interfacial breakage without forming a shear band [**Error! Reference source not found.**]. Crack path is thus determined by interfacial strength of the fiber/matrix interface in warp yarn region.

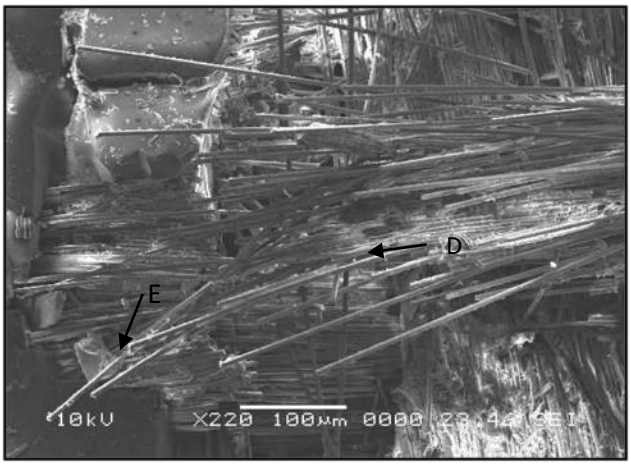

Figure 4. SEM micrograph of $[0°]_8$ specimen impacted at 10J.

Looking at the above SEM micrographs it is understood that *fiber pull out* is the major mechanism to absorb the impact energy. As the impact crack propagates, glass fibers are pulled out into loading direction and much impact energy is dissipated through this process.

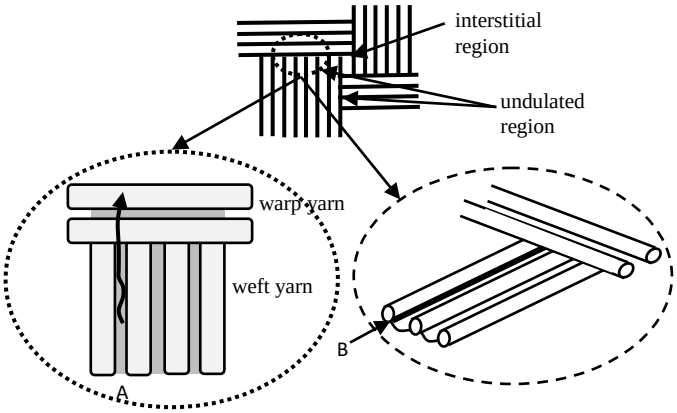

Figure 5. Schematic diagram of delamination mechanism [Redrawn from Error! Reference source not found. **,**Error! Reference source not found.**].**

To determine the characteristic damage state, the impacted $[0°]_8$ specimens were sectioned through the impact location in the direction parallel to the 0º fibers and observed under a low magnification microscope as seen in Fig. . As the impact energy increases the amount of deformation (curvature) extending through the thickness and the delamination (A) increased. A cone shape in the thickness direction with the in-plane damage area increasing from the impact surface to the bottom side is also observed. At 5J impact energy a nearly undamaged zone is visible inside this conical shape. At the bottom surface, the laminate suffers bending stress, which results in delamination and fiber failure.

Published By:
Blue Eyes Intelligence Engineering
and Sciences Publication (BEIESP)

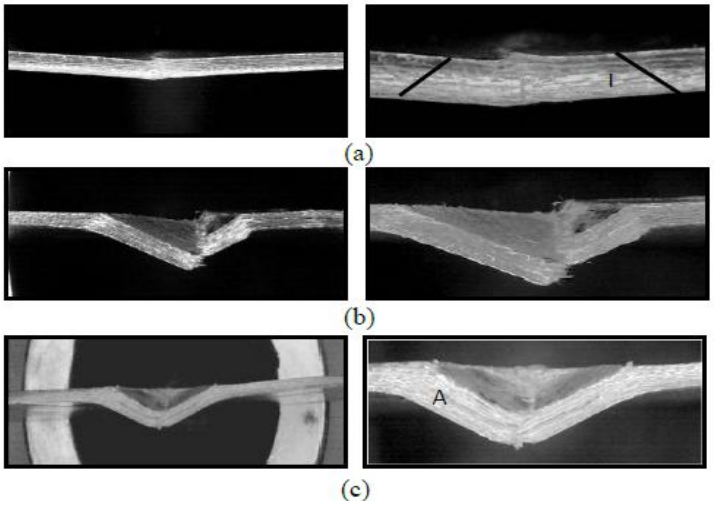

Fig. 6. Optical micrographs of polished cross sections of the center of impact for $[0°]_8$ specimen impacted at: (a) 5J (b) 7.5J (c) 10J, depicting pine tree (L) and Delamination (A)

16-Ply Laminates: Images of impact damage areas developed at different impact energies on the impact side and the bottom side of $[0^o]_{16}$ ply are shown in Figure 71.

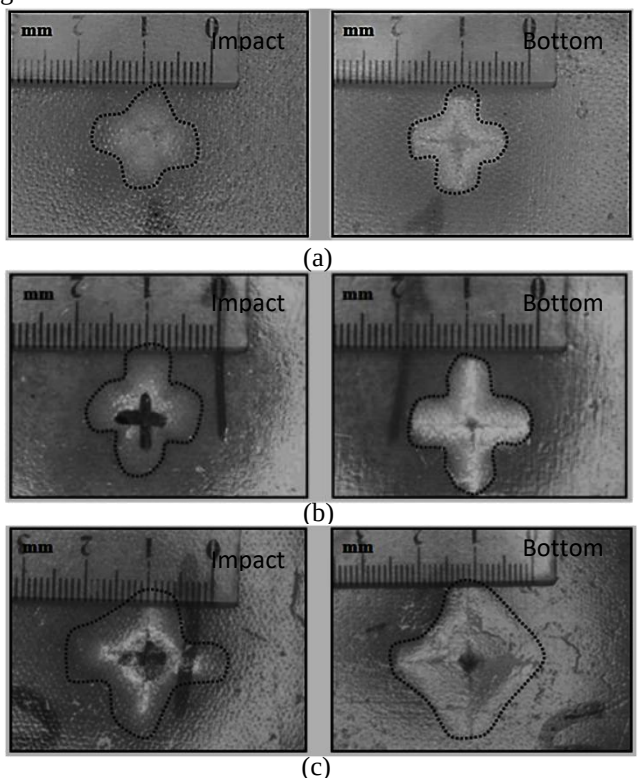

Figure 71. Impact and bottom side of the damage surface of $[0°]_{16}$ specimen impacted at (a) 5J (b) 7.5J (c) 10J

The progress of *crack* propagation at the bottom face of the specimen can be observed in Figure8 (a), which is schematically illustrated in Figure. Crack propagation in woven fabric composites considering its geometry is known to be rather complex when compared to that of non-woven unidirectional composites [**Error! Reference source not found.**]. In woven composites crack propagates parallel and as well as perpendicular to the fiber direction. The crack advances along the direction of fibers and as the crack propagation becomes rather unstable at a sudden load drop the whole crack front jumps forward across the perpendicular strand of fibers which is then immediately arrested at the next ripple forming a continuous crack front (see Figure). This is repeated until complete delamination of the laminate takes place.

Published By:
Blue Eyes Intelligence Engineering
and Sciences Publication (BEIESP)

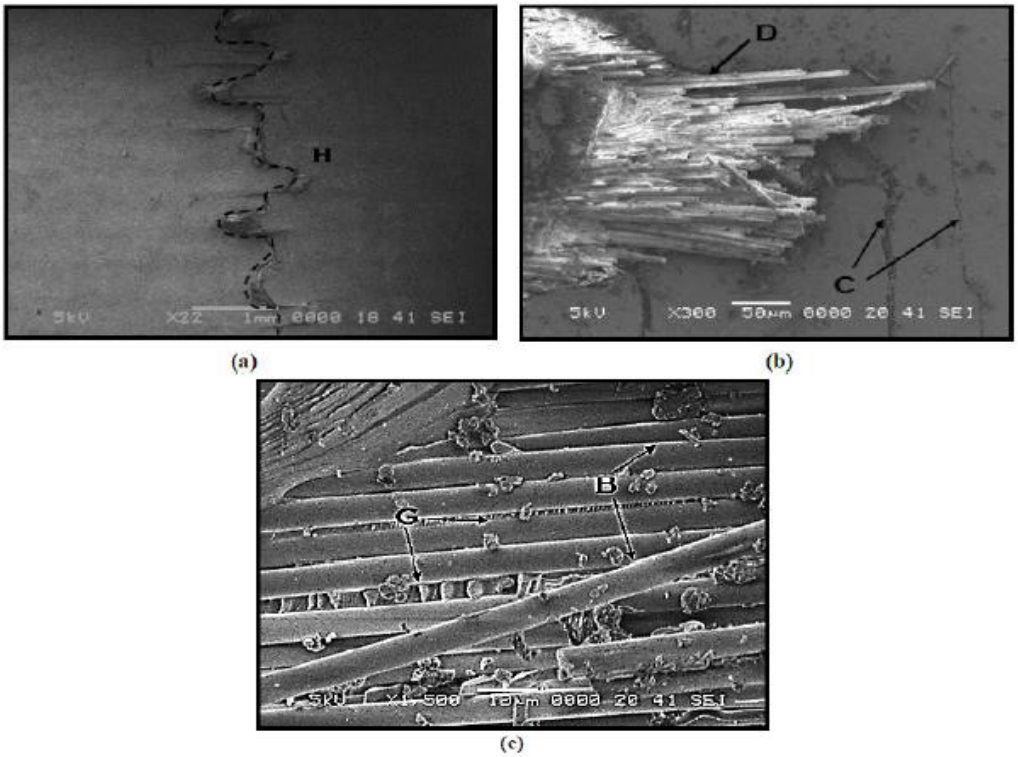

Figure 8. SEM micrographs of $[0°]_{16}$ specimen impacted at 5J depicting Fiber-Resin Debonding (B) Hackles (G).

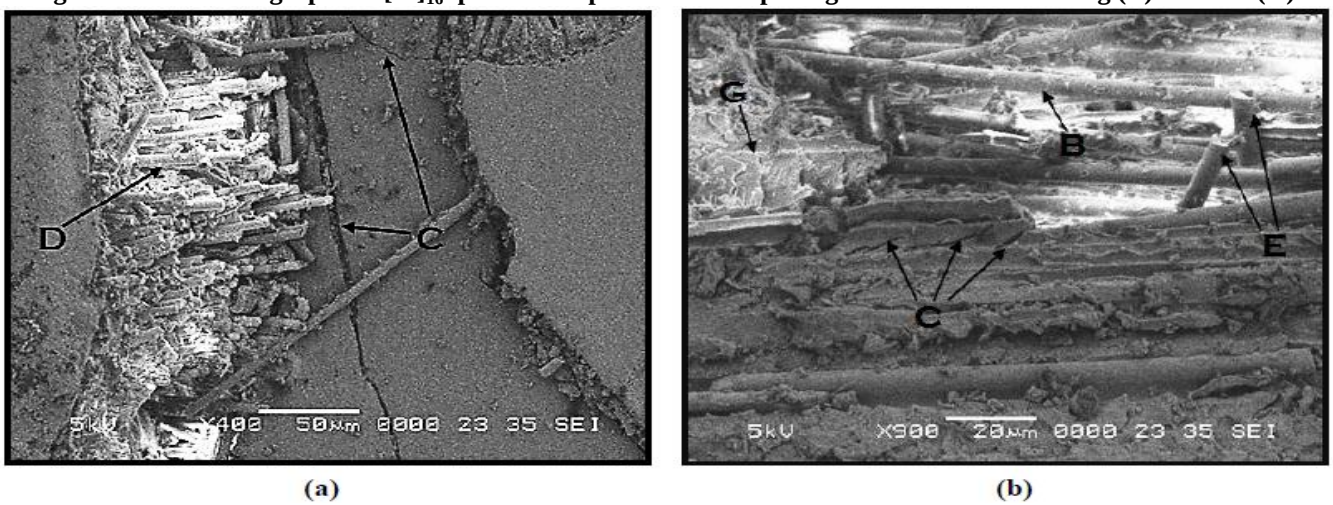

Figure 9. SEM micrograph of $[0°]_{16}$ specimen impacted at 7.5J depicting Fiber-Resin Debonding (B), Matrix Crack (C), Fiber Fracture (E) and Hackles (G).

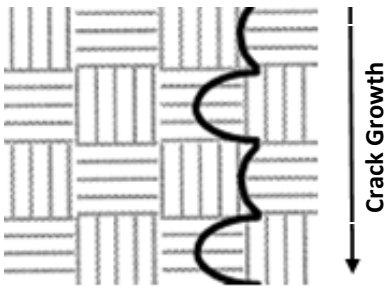

Figure 10. Delamination crack propagation in a woven-composite laminate [Error! Reference source not found.**].**

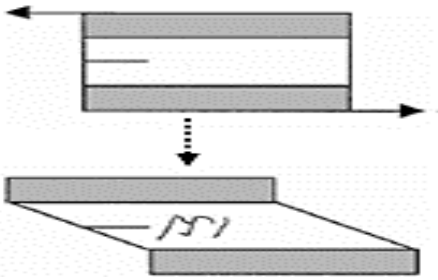

Figure 11. Schematic diagram of composite deformed under pure shear [Error! Reference source not found.**].**

Crack in woven composite could propagate through matrix and the fiber-matrix interface [**Error! Reference source not found.**]. A non-penetrating impact load as used in this current study causes predominantly mode II shear failure [**Error! Reference source not found.**] and the *hackle* structure is commonly observed in mode II failure [13].

Published By:
Blue Eyes Intelligence Engineering and Sciences Publication (BEIESP)

SEM micrographs in Figure (c), Figure 9 (b) and Figure (a, b) shows the formation of *hackles* at the fiber-matrix interface. During mode II shear deformation, as shown in Figure 11 each end under shear stress deforms in opposite direction, which leads stress to concentrate at the fiber-matrix interface, and as this stress increases a micro-crack is formed at the crack front in case if the interface is strong enough to endure the applied shear stress, and when the maximum effective stress at crack tip reaches the critical value, the micro-crack coalesce to from macro-crack and the macroscopic crack advances leading to *shear band* commonly known as hackles [13] as observed in this study. The formation of hackles increases with the increment of impact energy as observed from these SEM micrographs.

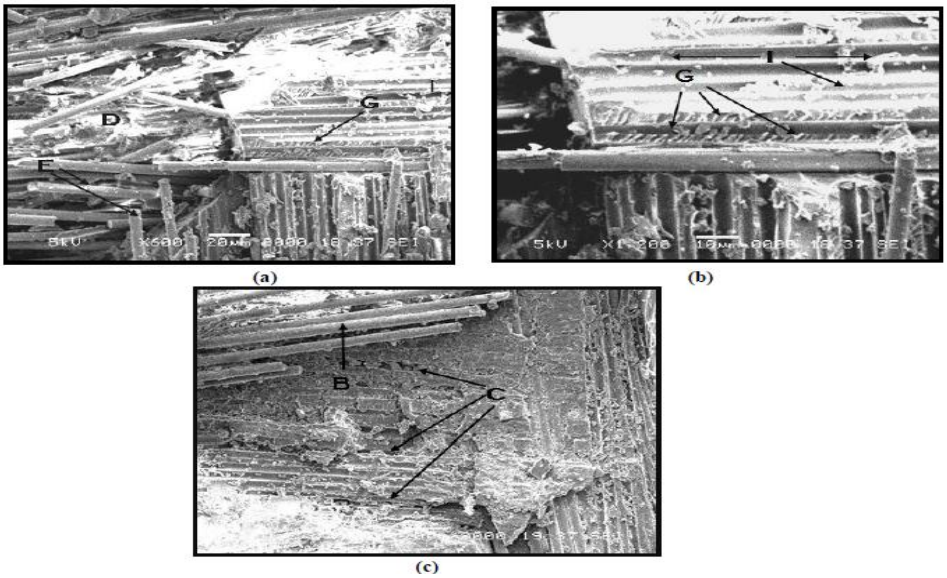

Figure 12. SEM micrographs of $[0°]_{16}$ specimen impacted at 10J.

The major failure mechanisms *debonding* and *fracture of matrix* (matrix cracks) are observed in SEM micrographs shown in Figure 9 and Figure (c) as well as increasing amount of *fiber fracture* with the increase of impact energy is observed in Figure 9 (b) and Figure (a). Bare fibers with little resin attached to them are separated from each other as the impact energy increased to 10J as seen in Figure (a), caused due to fiber-matrix debonding which also lead to extensive fragmentation of the matrix (*matrix debris*). The cross section view of impacted $[0°]_{16}$ specimen is shown in Figure. The warp and weft woven fibers did not restrict the formation of a cone-shape delamination zone (contrasted as white color) with increasingly extensive damage towards the bottom face as seen in Figure. The cone-shape delamination zone has been observed in various studies on non-woven composite laminates, but a similar phenomenon was also observed for woven-fabric composites. The cone or also known as the *pine tree* damage pattern comprised of delamination and had its apex at the top (near the point of impact) as shown in Figure (a) and a widening base through the thickness of the laminate as also shown schematically in Figure 14.

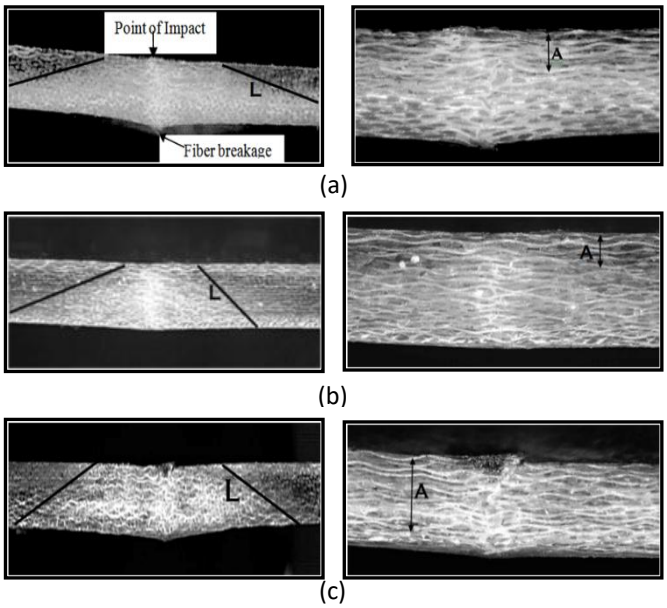

Figure 13. Optical micrographs of polished cross sections of the center of impact of $[0°]_{16}$ specimen impacted at: (a) 5J (b) 7.5J (c) 10J depicting pine tree (L) and Delamination (A)

Published By:
Blue Eyes Intelligence Engineering
and Sciences Publication (BEIESP)

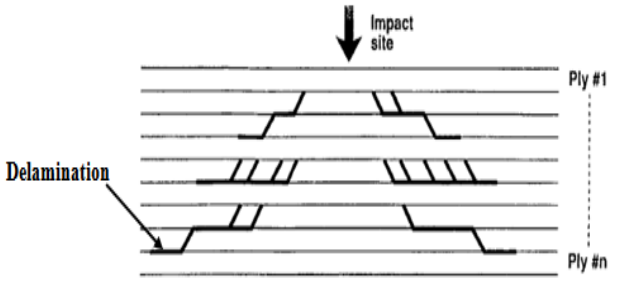

Figure 14. Schematic of cone of damage due to impact [13]

Fiber breakage at the bottom face of the specimen is noticeable in Figure 13(a) which results due to the tensile forces from bending. This process will continue with the increase in impact energy until complete perforation of the specimen occurs [**Error! Reference source not found.**]. The increment of the delamination depth is clearly evident with the ascending of the incipient impact energy on the specimens as shown in Figure (a)-(c).

24-Ply Laminates: With the increase of the material thickness as the number of plies increase from 16 to 24, there is significant decrease in the delamination area as seen in Figure. The impact damage of $[0°]_{24}$ specimen impacted at 5J as shown in Figure (a) is hardly visible on the impact side, therefore the internal delamination area of this specimen is lowest of all as shown in **Error! Reference source not found.**. As the damage of $[0°]_{24}$ specimen impacted at 5J was negligible, the SEM observation was unable to show any significant information. Mode-II shear failure is observed for the $[0°]_{24}$ specimens subjected to 7.5J of impact energy leading to debonding as observed from Figure. With the increase of impact energy the crack growth on the bottom ply can be seen in Figure (a). Unlike to $[0°]_{16}$ specimen, formation of hackles in a $[0°]_{24}$ specimen was considerably less at 10J impact energy as seen at higher magnifaction as shown in Figure possibly due to weak fiber-matrix interfacial strength [**Error! Reference source not found.**] which lead to fiber-matrix debonding which remains as major failure mechanism at this stage as seen in Figure (b).

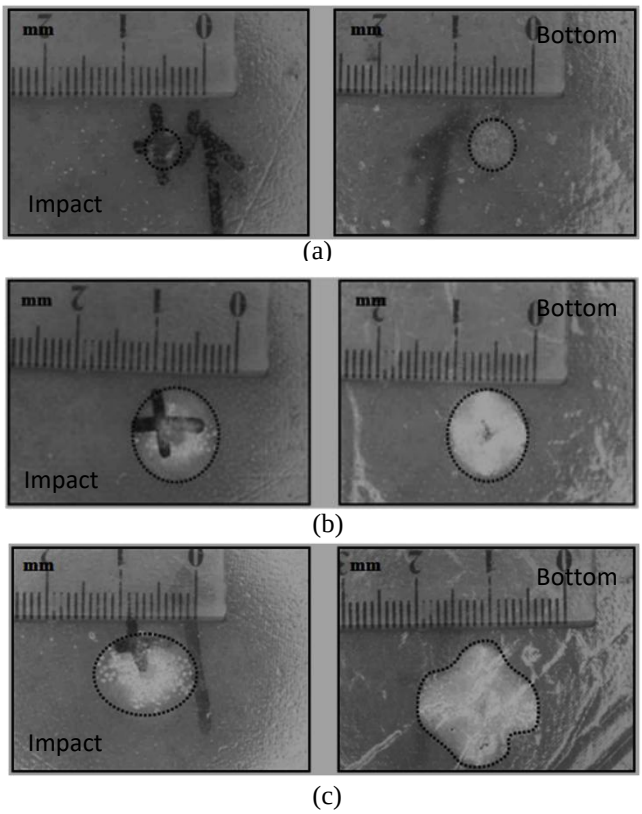

Figure 14. Impact and bottom side of the damage surface of $[0°]_{24}$ specimen impacted at (a) 5J (b) 7.5J (c) 10J

Published By:
Blue Eyes Intelligence Engineering
and Sciences Publication (BEIESP)

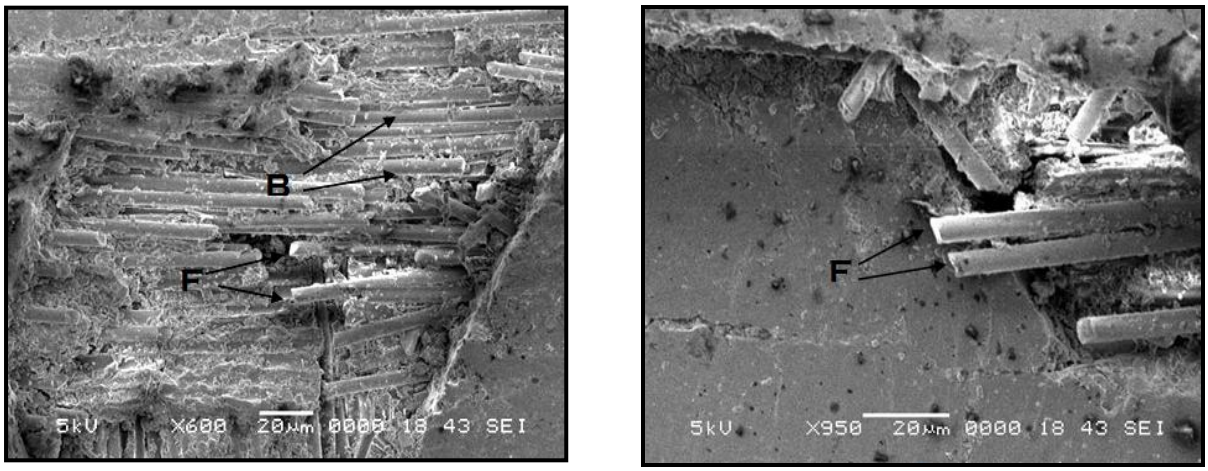

(a) **(b)**

Figure 15. SEM micrographs of $[0°]_{24}$ specimen impacted at 7.5J.

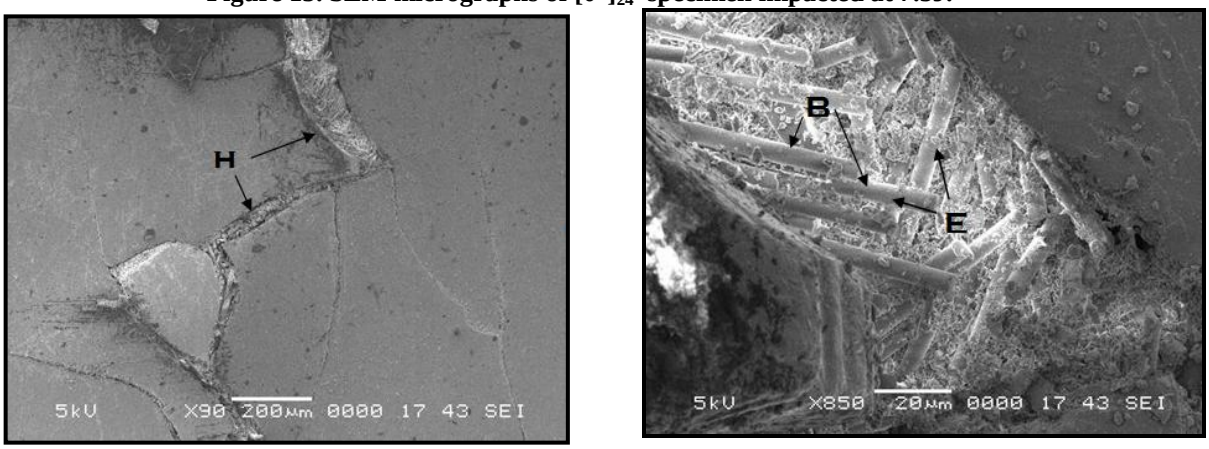

(a) **(b)**

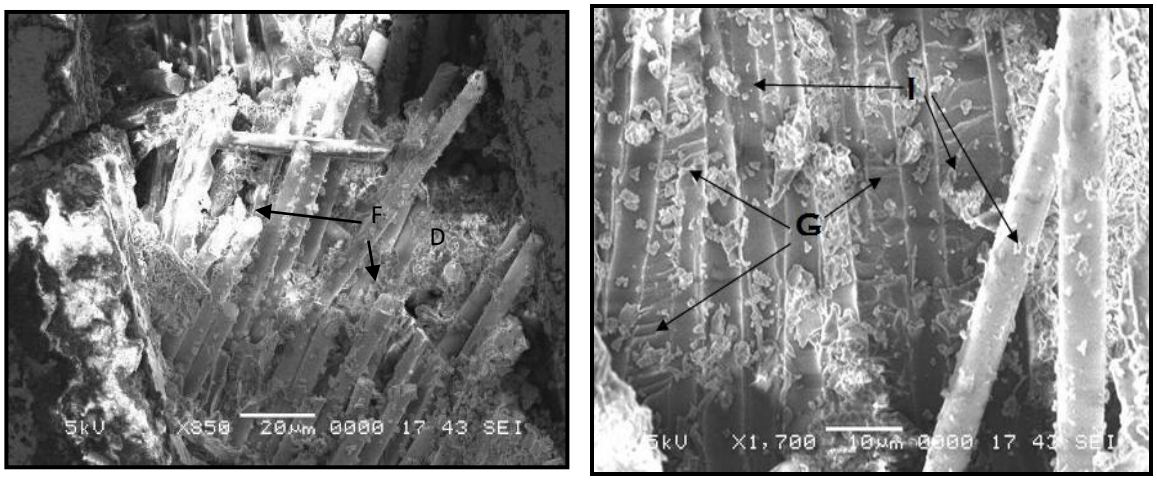

(c) (d)

Figure 16. SEM micrograph of $[0°]_{24}$ specimen impacted at 10J depicting formation of Hackles (G) and Debris of Resin (I).

Published By:
Blue Eyes Intelligence Engineering
and Sciences Publication (BEIESP)

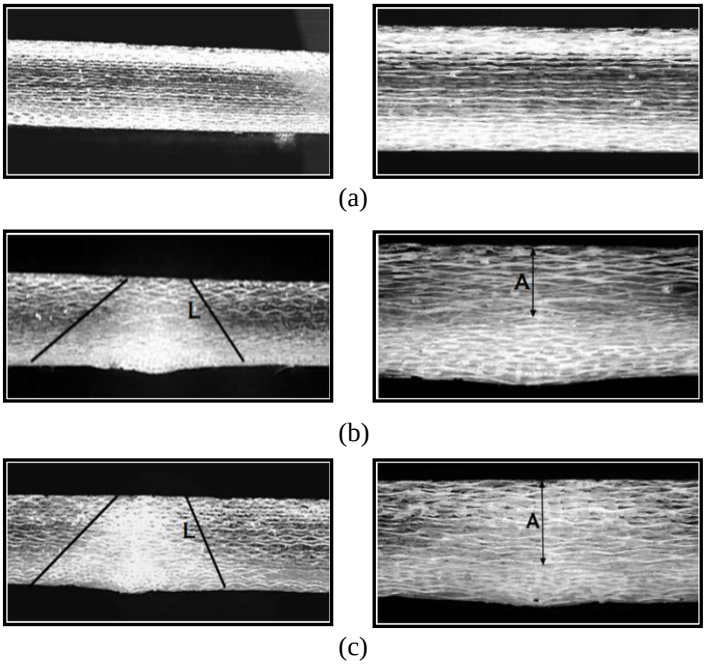

Figure 17. Optical micrographs of polished cross sections of the center of impact of $[0°]_{24}$ specimen impacted at: (a) 5J (b) 7.5J (c) 10J, depicting pine tree (L) and Delamination (A)

As learned before the damage at 5J impact energy was negligible, therefore *pine tree* damage pattern is not visible in the cross sectional view as seen in Figure (a) but later as the impact energy increased the progress of delamination is observed from Figure (b) and (c) within the cone of damage.

32-Ply Laminates: The images taken by low magnification microscope, showing the progress of impact damage at the front and bottom face of the $[0°]_{32}$ specimen with the increase of incident impact energy (see Figure). As can be observed the damage at the bottom face of the material is larger than that of the impacted side which could be explained as the delamination progress through the plies forming a cone of damage. The shape of the damage at the bottom face remains nearly circular.

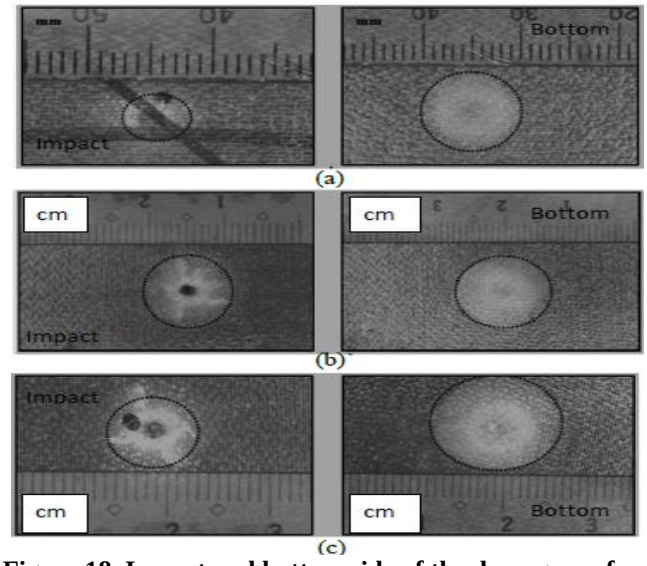

Figure 18. Impact and bottom side of the damage surface of $[0°]_{32}$ specimen impacted at (a) 5J (b) 7.5J (c) 10J

Unlike the 16 and 24 ply specimen, damage at the bottom side of 32 ply specimen didn't show the formation of crack (as seen in Figure (a) and Figure (a)), instead small local damage areas were formed at all impact energies used. The reason could be related to the incident impact energy being unable to cause much of the delamination reach the lowest ply i.e. 32nd ply. Observing the local damage areas at higher magnifications, one could observe the fiber failure at the bottom ply and local delamination between the outer (lowest) and the inner ply (see Figure), and as the impact energy was increased to 10J the failure of the fibers at the outer ply increased as seen in Figure.

Published By:
Blue Eyes Intelligence Engineering
and Sciences Publication (BEIESP)

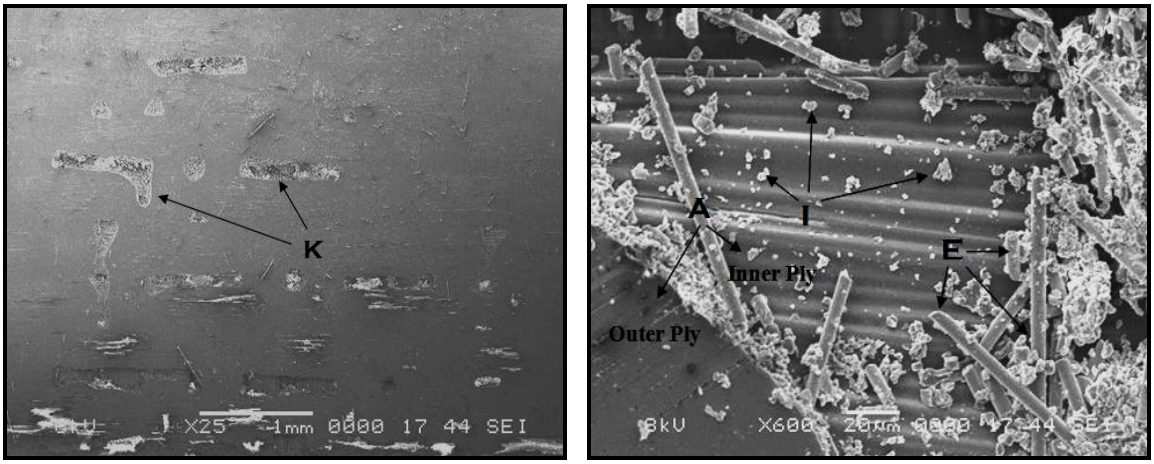

(a) (b)

Figure 19. SEM micrographs of $[0°]_{32}$ specimen impacted at 5J.

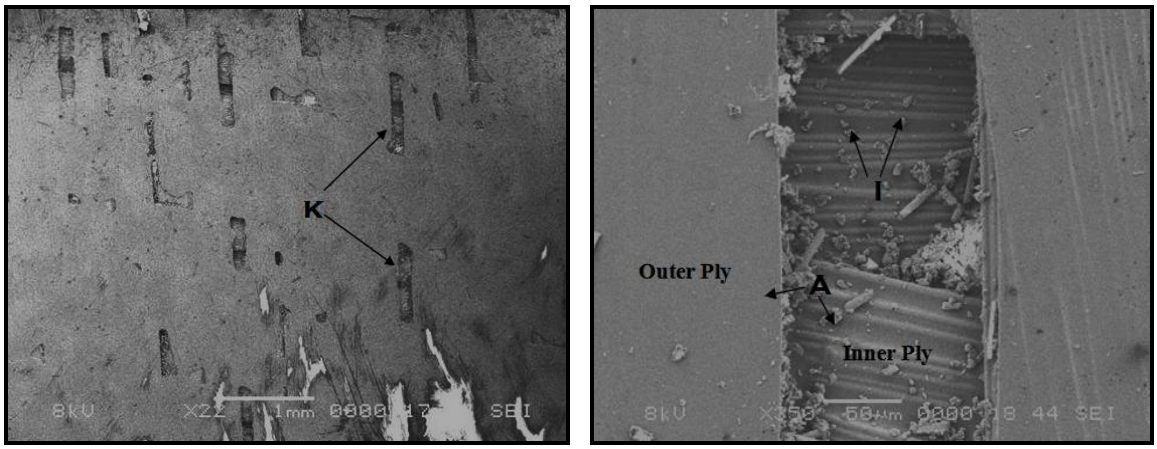

(a) (b)

Figure 20. SEM micrographs of $[0°]_{32}$ specimen impacted at 7.5J.

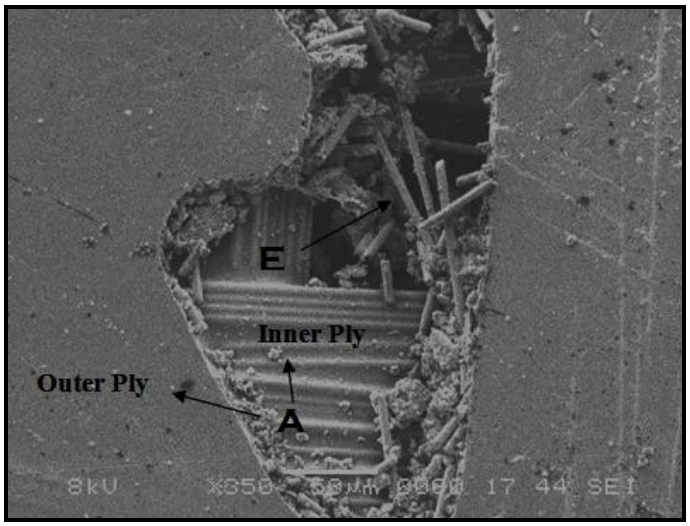

Figure 21. SEM micrograph of $[0°]_{32}$ specimen impacted at 10J.

Published By:
Blue Eyes Intelligence Engineering
and Sciences Publication (BEIESP)

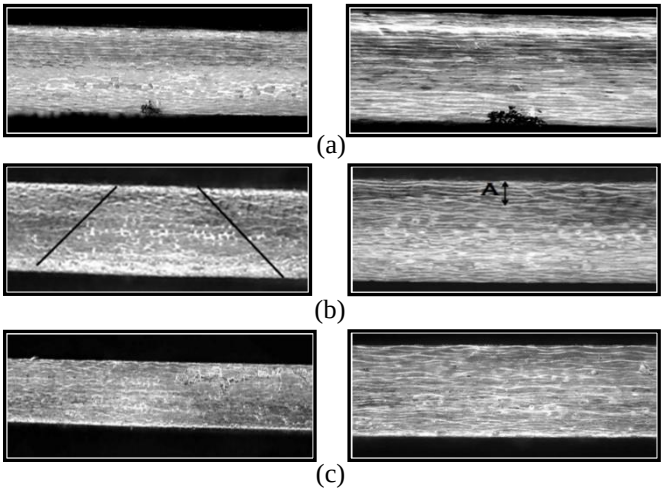

Figure 22. Optical micrographs of polished cross sections of the center of impact of $[0°]_{32}$ specimen impacted at: (a) 5J (b) 7.5J (c) 10J, depicting pine tree (L) and Delamination (A)

The cross section view of impacted $[0°]_{32}$ ply specimen, shows very little amount of delamination and even the progress of delamination through the thickness is hardly visible (see Figure). SEM and optical observations were unable to explain the phenomenon of internal damage to this specimen.

IV. CONCLUSIONS

One of the important factors to consider in failure of woven fabric composites is the *resin rich regions*. These resin rich regions are formed at two different positions, namely the interstitial region and the undulated region. An interstitial region is surrounded by 4 yarns (see Figure) and the undulated region is formed at the intersection of warp and weft yarns. These resin rich regions are potential sources for the weakness of a woven composite structure.

In this study it was found that under local stress due to impact the interstitial region of 0° woven glass fiber reinforced composite laminates fail by matrix cracking. These matrix cracks were denser in thin 8 ply composite than compared to the thicker 16, 24 and 32 ply laminates. The matrix cracks propagate to cause fiber pull out (fiber matrix debonding) and fiber fracture. The matrix cracks formed in the undulated region extend across the thickness of the laminate to introduce delamination. The eventual non-penetration failure of the composite laminates thus occurred by a combination of matrix cracking, fiber pull out and fracture and delaminating.

ACKNOWLEDGEMENT

The author wish to thankfully acknowledge the support of King Fahd University of Petroleum and Minerals and Saudi Aramco for funding this research through research project ME 2236

REFERENCES

1. N. R. Mathivanan, J. Jerald, “Experimental Investigation of Woven E-Glass Epoxy Composite Laminates Subjected to Low-Velocity Impact at Different Energy Levels”, Journal of Minerals & Materials Characterization & Engineering, Vol. 9, No.7, 2010, pp.643-652,
2. Ben Jar, Gros X E, Takahashi K, Kawabatta K, Murai J, Shinagawa Y, Evaluation of Delamination Resistance of Glass Fibre Reinforced Polymers Under Impact Loading, Journal of Advanced Materials, July 2000, Vol. 32, No. 3, pp. 35-45
3. L. Sunith Babu, H. K. Shivanand, “SEM Based Studies on Damage Analysis of GFRP and CFRP Sandwich Composites” American Journal of Materials Science 2015, 5(3C), pp. 146-150
4. M.T.H.Sultan, A.Hodzic, W.J.Staszewski and K. Worden, “A SEM-Based Study of Structural Impact Damage”, Applied Mechanics and Materials Vols. 24-25 (2010) pp. 233-238
5. T. Lendze, R. Wojtyra, L. Guillaumat, C. Biateau, K. Imielińska, “Low Velocity Impact Damage in Glass/Polyester Composite Sandwich Panels, Advances in Materials Science, Vol. 6, No. 1 (9), 2006, PP. 26-35
6. Tien-Wei Shyr, Hao Pan Yu, Impact resistance and damage characteristics of composite laminates, Composite Structures, 2003, Vol. 62, pp. 193–203.
7. Dahsin Liu, Delamination resistance in stitched and unstitched composite plates subjected to Impact Loading, Journal of Reinforced Plastics and Composites, January 1990, Vol. 9.
8. Sohn M.S., Hua X.Z, Kimb J.K, and Walkera L, Impact damage characterization of carbon fibre/epoxy composites with multi-layer reinforcement, Composites: Part B, 2000, Vol. 31, pp. 681-691
9. Morais W.A de, Monteiro S.N, d’ Almeida J.R.M, Effect of the laminate thickness on the composite strength to repeated low energy impacts, Composite Structures, 2005, Vol. 70, pp. 223–228.
10. Dear, J. P., Brown, S. A., Impact Damage Processes in Reinforced Polymeric Materials, Composites Part A: Applied Science and Manufacturing 34 pp. 411-420, 2003.
11. Chang, F., and Y. Choi, “Damage of laminated Composites due to Low-velocity impact”, Mechanics of Materials, Vol. **10**, (1990), p. 83.
12. Zhou, G., “Damage resistance and tolerance in thick laminated composite plates subjected to low-velocity impact,” *Key Engineering Materials*, **141-143**, (1998), pp.305-334.
13. M.S. Found, "Impact Behaviour of FRP Composites", Key Engineering Materials, Vol. 144, pp. 55-62, Sep. 1997

Published By:
Blue Eyes Intelligence Engineering and Sciences Publication (BEIESP)